Journal of Medicinal Chemistry

Article

Discovery and Structure-Activity Relationship of a Bioactive Fragment of ELABELA that Modulates Vascular and Cardiac Functions

Alexandre Murza, Xavier Sainsily, David Coquerel, Jérôme Côté, Patricia Marx, Élie Besserer-Offroy, Jean-Michel Longpre, Jean Lainé, Bruno Reversade, Dany Salvail, Richard Leduc, Robert Dumaine, Olivier Lesur, Mannix Auger-Messier, Philippe Sarret, and Eric Marsault

J. Med. Chem., **Just Accepted Manuscript** • DOI: 10.1021/acs.jmedchem.5b01549 • Publication Date (Web): 17 Mar 2016

Discovery and Structure-Activity Relationship of a Bioactive Fragment of ELABELA that Modulates Vascular and Cardiac Functions

Alexandre Murza,[§,¥] Xavier Sainsily,[§,¥] David Coquerel,[#] Jérôme Côté,[§,¥] Patricia Marx,[§,¥] Élie Besserer-Offroy,[§,¥] Jean-Michel Longpré,[§,¥] Jean Lainé,[§] Bruno Reversade,[&] Dany Salvail,[†] Richard Leduc,[§,¥] Robert Dumaine,[§] Olivier Lesur,[#] Mannix Auger-Messier,[#] Philippe Sarret[§,¥,$] and Éric Marsault[§,¥,$,*]

[§] Département de Pharmacologie et Physiologie, Faculté de Médecine et des Sciences de la Santé, Université de Sherbrooke, Sherbrooke, J1H 5N4, Québec, Canada

[#] Département de Médecine, Faculté de Médecine et des Sciences de la Santé, Université de Sherbrooke, Sherbrooke, J1H 5N4, Québec, Canada

[†] IPS Thérapeutique Inc., Sherbrooke, J1G 5J6, Québec, Canada

[&] Laboratory of Human Embryology & Genetics, Institute of Medical Biology, A*STAR, 8A Biomedical Grove, 138648, Singapore

[¥] Institut de Pharmacologie de Sherbrooke, Sherbrooke, J1H 5N4, Québec, Canada

KEYWORDS: ELABELA, APELA, Toddler, APLNR, apelin, APJ, inotrope, cardiovascular diseases.

ABSTRACT

ELABELA (ELA) was recently discovered as a novel endogenous ligand of the apelin receptor (APJ), a G protein-coupled receptor. ELA signaling was demonstrated to be crucial for normal heart and vasculature development during embryogenesis. We delineate here ELA's structure-activity relationships and report the identification of analogue **3** (ELA(19-32)), a fragment of ELA that binds to APJ, activates the $G\alpha_{i1}$ and β-arrestin-2 signaling pathways and induces receptor internalization similarly to its parent endogenous peptide. An alanine scan performed on **3** revealed that the C-terminal residues are critical for binding to APJ and signaling. Finally, using isolated-perfused hearts and *in vivo* hemodynamic and echocardiographic measurements, we demonstrate that ELA and **3** both reduce arterial pressure and exert positive inotropic effects on the heart. Altogether, these results present ELA and **3** as potential therapeutic options in managing cardiovascular diseases.

INTRODUCTION

The Apelin receptor (APJ, APLNR or angiotensin receptor like-1), isolated from bovine stomach extracts in 1993, is a member of the class A G protein-coupled receptor (GPCR) superfamily and shares 30% homology with the angiotensin II receptor type 1 (AT_1).[1] Its endogenous ligand, apelin, was isolated in 1998 and found to circulate under several isoforms highly conserved among vertebrates.[2,3] Its 77-residue precursor, pre-pro-apelin, undergoes proteolytic cleavages to ultimately produce apelin-36, -17, and -13 (or its pyroglutamate analogue Pyr1-apelin-13), the latter being the major form in circulation.[4] The apelinergic system is widely distributed in peripheral tissues, particularly the heart, lung, kidney and pancreas, as well as the central nervous system, especially the hypothalamus and spinal cord.[5–8] In the last decade, various physiological functions were associated with the apelinergic system,[3] such as the regulation of fluid homeostasis,[9,10] the modulation of the cardiovascular system,[11–13] and the regulation of energy metabolism.[14,15] At the cellular level, the activation of APJ triggers a variety of G protein-dependent signaling pathways, including inhibition of adenylate cyclase which translates in reduced cyclic adenosine monophosphate (cAMP) levels, calcium mobilization, phosphorylation of extracellular signal-regulated kinases 1/2 (ERK1/2) and p70S6K as well as nitric oxide synthase (NOS) activation.[8,16–19] Different isoforms of apelin were also shown to recruit β-arrestin-1 and β-arrestin-2, inducing internalization of the APJ receptor through different intracellular trafficking routes.[20] The structure-function relationship of apelin remains unclear and is the subject of a growing body of literature. However, several studies recently demonstrated that the C-terminal Phe13

amino acid is a molecular determinant of the hypotensive action of apelin-13,[21–23] plasma stability,[24–26] and APJ internalization/β-arrestin recruitment.[27,28]

For more than a decade, apelin (under its various isoforms) was the only known endogenous ligand of APJ, until the discovery in 2013 of a new peptide named ELABELA (ELA, www.elabela.com, also known as Toddler, Apela or APJ early endogenous ligand) in a conserved region of the human genome believed to be non-coding.[29,30] The observation that knockout of *Apelin* in zebrafish or mice did not reproduce the phenotype of the *Apj* knockout suggested the possible existence of another endogenous ligand.[29–31] Apj and Ela mutants in zebrafish display very similar phenotypes, suggesting they may be biologically linked. Initially translated as a 54 amino-acid peptide, the mature form of ELA contains 32 amino acids, ELA(1-32) (**Figure 1**; to be noted, throughout this manuscript, numbering of ELA refers to numbering of the secreted peptide ELA(1-32), and not to numbering of the full-length protein).[29] Contrary to the wide distribution of apelin and APJ, ELA is mainly found in human embryonic stem cells and in adult kidney and prostate.[32] Ela mutations have been broadly studied in zebrafish to determine its role in early embryonic development. Recessive, loss-of-function mutant Ela alleles have been generated in zebrafish, resulting in a defective mature Ela protein. A striking feature of homozygous mutant Ela zebrafish was either the presence of a rudimentary heart or complete heart agenesis.[29,30,33] Thus, ELA appears to be crucial for normal heart and vasculature development during embryogenesis. Furthermore, during vasculogenesis, the migration of angioblasts expressing APJ is mainly triggered by ELA, which underscores its role in angiogenesis *in vivo*.[34] In accordance, ELA has been shown to stimulate angiogenesis of human umbilical

vascular endothelial cells (HUVECs) through activation of APJ, and induces relaxation of mouse aortic blood vessels.[32] In contrast to apelin, ELA triggers relaxation of blood vessels even when pre-treated with L-NAME (nitric oxyde (NO) synthase inhibitor), suggesting that NO is not required for ELA-mediated vascular relaxation.[32]

The primary sequence of ELA is highly conserved in vertebrates, particularly on its C-terminal portion.[29,30] To date, the signaling pathways associated with ELA remain poorly elucidated. It was shown that ELA promotes the rapid internalization of APJ, inhibits cAMP accumulation, activates ERK1/2 phosphorylation and weakly induces intracellular calcium mobilization.[32] In adult male Sprague-Dawley rats, ELA regulates fluid homeostasis by increasing water intake and diuresis, similarly to apelin.[35] Alanine substitution of the C-terminal Pro residue led to the discovery of an antagonist of the ERK pathway following activation by apelin or ELA, additionally decreasing urine flow rate and water intake after intraperitoneal administration to rats.[35] Ho *et al* reported that ELA possesses potent signaling activity in human embryonic stem cells (hESCs), where it is abundantly secreted. Strikingly, these pluripotent cells do not express APJ but readily activate the PI3K/AKT pathway when stimulated by synthetic full-length ELA. These results suggest the existence of yet another cell surface receptor for ELA in hESCs.[36]

The structure-activity relationship (SAR) of ELA for its receptor APJ and comparisons with the known SAR of apelin remain to be elucidated. Moreover, to explore the full therapeutic potential of ELA, it is important to decipher the key pharmacophores of this 32-mer peptide, with the additional goal to reduce its size. In this manuscript, we report the identification of a significantly smaller bioactive fragment of ELA, ELA(19-32), that binds to APJ in the nM range and activates several signaling

pathways similarly to that of the two endogenous ligands apelin-13 and ELA. Furthermore, we also provide the first alanine scan of this ELA analogue, as well as the identification of key residues involved in binding and signaling. Finally, we demonstrate that ELA and its active (19-32) fragment increase the left ventricular developed pressure (LVDP) in the isolated-perfused rat heart and induce strong hypotensive effects *in vivo* in rats.

RESULTS AND DISCUSSION

Synthesis

Peptides were synthesized on solid phase using the Fmoc strategy. The first Fmoc N-protected C-terminal residue was attached to the 2-chlorotrityl chloride resin (loading of 0.25 mmol/g) in the presence of *N,N*-diisopropylethylamine (DIPEA) in dichloromethane (DCM). Capping of unreacted 2-chlorotrityl chloride groups was carried out with a mixture of DCM/MeOH/DIPEA (7/2/1). The Fmoc group was then cleaved with piperidine/*N,N*-dimethylformamide (DMF, 1/4). The following Fmoc N-protected amino acids were then coupled stepwise in the presence of [O-(7-azabenzotriazol-1-yl)-1,1,3,3-tetramethyluronium hexafluorophosphate] (HATU) and DIPEA in DMF. The resin was cleaved then side-chains were simultaneously deprotected with a mixture of TFA (trifluoroacetic acid)/H_2O/TIPS (triisopropylsilane)/1,2-ethanedithiol (EDT) (92.5/2.5/2.5/2.5). The disulfide bridge between the two cysteine residues was formed in oxidative conditions using I_2 (iodine) in an acetic acid/H_2O mixture (70%), then the crude was lyophilized. Uncyclized analogues were directly precipitated in *tert*-butyl methyl ether (TBME) then purified by reverse-phase chromatography, leading to the desired compounds with >95% purity as determined by Ultrahigh Performance Liquid Chromatography-Mass spectrometry (UPLC-MS) and characterized by High Resolution Mass Spectroscopy (HRMS). Compounds **9** and **12** are >94% pure and compound **14** is >93% pure.

Proteolytic degradation of ELA and identification of a bioactive fragment

Two pairs of dibasic amino acids Arg9-Arg10 and Arg20-Arg21 of the ELA mature peptide suggest possible cleavage by pro-hormone convertases (**Figure 1**).[29] In order to examine the susceptibility of ELA to proteolytic cleavage and identify shorter active fragments, ELA was incubated with rat plasma during two hours at 37°C. In these conditions, the production of two peptides was observed by UPLC-MS: ELA(1-9) (M_w 1098.3 Da) and ELA(11-32) (M_w 2715.3 Da), confirming the occurrence of a rapid cleavage between residues Arg9-Arg10 and Arg10-Lys11 (**Figure 1**). Similarly to apelin-13 (half-life ~ 4 min in these conditions), the plasma half-life of ELA was very short, and after 2 minutes of incubation the parent compound was almost completely degraded (Supporting Information, Figure S2). Consistently, analogue **3** (ELA(19-32)) was also rapidly metabolized in rat plasma ($t_{1/2} < 2$ min).

The key apelin-13 pharmacophores are the N-terminal Arg2 and Arg4 residues and the C-terminal Phe13 residue.[22,27,37] Comparison of these pharmacophoric elements with the primary structure of ELA suggest that a shorter fragment of ELA could bind APJ (**Figure 1**). Therefore, we synthesized peptide **1** (ELA(17-32)), which retains the disulfide bridge, analogue **2** which possesses the corresponding free cysteine residues, as well as shorter analogues **3** (ELA(19-32)) and **4** (ELA(22-32)) (**Table 1**). It should be noted that the N-terminal Gln residue in **3** was replaced by a pyroglutamic acid (Pyr) residue, similarly to Pyr1-apelin-13.[25] This modification, often found in bioactive peptides, stabilizes and protects against N-exoproteases.[38] Compounds **1**-**3** (K_i 0.23 nM, 0.34 nM and 0.93 nM, respectively) exhibited binding affinities comparable to that of ELA (K_i 0.19 nM) and apelin-13 (K_i 0.37 nM). However, analogue **4** (K_i 14 nM)

exhibited a 75-fold loss in affinity versus ELA, suggesting that **3** contains key pharmacophoric features required to interact with APJ, similar to the parent peptide. Furthermore, these results suggest that the macrocyclic nature of ELA is not essential for binding to APJ.

The ability of new analogues to activate the $G\alpha_{i1}$ pathway as well as β-arrestin-2 recruitment was then assessed using bioluminescence resonance energy transfer (BRET) assays (**Table 1**).[39,40] Upon binding, ELA triggers $G\alpha_{i1}$ (EC_{50} 5.3 nM) and β-arrestin-2 (EC_{50} 45 nM) signaling with potencies close to that of apelin-13 (EC_{50} 1.9 nM and 68 nM, respectively). Analogues **1**-**3** exhibited similar potencies compared to ELA, while the shortest analogue **4** led to a 10-fold decrease in β-arrestin-2 recruitment efficacy. From these results, **3** emerges as a smaller, yet still potent bioactive fragment of ELA.

Previous studies have revealed that internalization and signaling of the APJ receptor are functionally dissociated, as exemplified by analogues in which the C-terminal Phe residue is truncated or substituted with Ala.[21,27] Furthermore, the ability of the apelin fragments to induce APJ internalization has been linked to their efficacy at lowering blood pressure.[21] Accordingly, we evaluated the ability of ELA and analogue **3** to induce receptor internalization. The cell surface expression of HA-tagged human APJ was followed by ELISA assay, revealing that analogue **3** is slightly less potent than apelin-13 and ELA to elicit receptor internalization (EC_{50} 36 nM, 16 nM and 10 nM, respectively) (**Figure 2**). Shorter fragment **4** was found to be less prone to induce APJ internalization by more than one order of magnitude (EC_{50} 476 nM), in agreement with its weaker potency to elicit β-arrestin-2 recruitment.

Alanine scan of analogue 3

In order to identify the key pharmacophoric elements in analogue **3**, we carried out an alanine scan. The resulting analogues were first evaluated for their ability to bind the APJ receptor (**Table 2**). In this series, the replacement of the C-terminal moiety of compound **3** with Ala (i.e. residues Arg28, Val29, Pro30, Phe31 and Pro32) resulted in the highest loss in binding affinity compared to **3**. Indeed, replacement of Pro30 or Phe31 by Ala provided a 50-fold loss (**7**, K_i 48 nM; **6**, K_i 49 nM vs. **3**, K_i 0.93 nM), whereas the Arg28Ala substitution led to a drastic 175-fold deterioration in binding affinity (**9**, K_i 164 nM). At a similar position in apelin-13, the substitution of residue Lys8 by Ala led to a minor decrease in affinity (< 10-fold).[8] These dissimilarities suggest different interactions of the cationic side-chains of apelin-13 and ELA with the APJ receptor. This opens up an interesting avenue to optimize the affinity of the newly identified fragment of ELA. Interestingly, Ala replacement of Pro32 led to a >10-fold decrease in affinity (**5**, K_i 11 nM vs. **3**, K_i 0.93 nM). Proline and glycine residues are structurally important since they can stabilize turn conformations which can be critical for molecular recognition.[41] In the present case, the position of Pro32 at the C-terminal end of the peptide makes it unlikely to profoundly influence the conformation of ELA. A possible hypothesis to explain this substantial decrease in affinity could be related to a change in the orientation of the carboxylic acid group resulting from the Pro32Ala replacement. Therefore, it appears that the orientation of the negative charge in the C-terminal binding pocket of APJ is of importance. This hypothesis is consistent with the observation that the C-terminal amide derivative **19** also exhibited a >10-fold loss in binding affinity compared to **3** (**19**, K_i 22 nM). This is also congruent with previous SAR on apelin-13 reporting that deletion or

structural modifications in the C-terminal Phe13 residue deeply impacted binding affinity.[8,23,25]

Analogue His26Ala provided a 40-fold decrease in affinity compared to **3** (**11**, K_i 35 nM vs. **3**, K_i 0.93 nM). This is in sharp contrast with the results of the Ala scan published by Medhurst and coworkers, who reported a mild increase in binding for His7Ala mutation of apelin-13.[8] Indeed, His residues in apelin-13 and analogue **3** are located in the central moiety of the peptide, at almost identical positions. His26 side chain of compound **3** may make crucial interactions for binding with APJ, which cannot be reached by apelin-13. When replaced by Ala, the two lipophilic residues Leu25 and Val29 of ELA(19-32) led to a 20-fold decrease in binding affinity compared to the parent peptide (**12**, K_i 20 nM; **8**, K_i 20 nM) (**Table 2**).

Contrary to the C-terminal end, the six N-terminal amino acids of analogue **3** seem to be less critical for APJ interactions. Ala mutations elicited a minor drop in binding (compounds **13** to **18**; K_i 0.53 to 8.4 nM), in sharp contrast with apelin-13 in which the Arg2-Pro3-Arg4-Leu5-Ser6 moiety plays a key role.[42,43] Interestingly, the Pro24Ala modification did not affect affinity (**13**, K_i 4.0 nM), suggesting that Pro24 is less structurally important in **3** than in apelin-13. To be noted, Pro24 is not entirely conserved phylogenetically and is replaced by a serine residue in rat ELA. Additionally, while both Arg residues of apelin-13 are important for binding, this is not the case for residues Arg20 and Arg21 of **3** since their replacement by Ala does not alter affinity (**16**, K_i 6.8 nM; **17**, K_i 8.4 nM).

Finally, to circumvent oxidation by-products often associated with the presence of Met or Cys residues in peptides,[44] we synthesized Cys22Ser and Met23Nle derivatives of

3. Both modifications had a marginal effect on affinity compared to the parent peptide (**20**, K_i 0.37 nM; **21**, K_i 0.14 nM). Overall, these results reveal important differences concerning the key pharmacophores of compound **3** compared to those of apelin-13, and suggest that the two peptides interact in different ways in the orthosteric binding pocket of APJ.

Effects of Ala substitutions on $G\alpha_{i1}$ activation and β-arrestin-2 recruitment

The ability of the above Ala-substituted analogues to activate $G\alpha_{i1}$ dissociation and β-arrestin-2 recruitment was then assessed using BRET biosensors (**Table 2**).[39,40] Overall, the potency of the new analogues on these two signaling pathways followed the trends observed in binding assays. Indeed, the Arg28, Val29, Pro30, Phe31 residues, which exhibited the most important drop in affinity when replaced by Ala, also provided a substantial decrease in signaling, especially regarding β-arrestin-2 recruitment (**6**, **7**, **8** and **9**; EC_{50} 1250 nM to >10 μM). Interestingly, analogue **5** led to similar potencies compared to **3** (**5**, $G\alpha_{i1}$, EC_{50} 12 nM; β-arr2, EC_{50} 266 nM vs. **3**, $G\alpha_{i1}$, EC_{50} 8.6 nM; β-arr2, EC_{50} 166 nM), while possessing a 10-fold lower affinity. However, the C-terminal amide derivative (compound **19**) activated the $G\alpha_{i1}$ pathway with slightly lower potency compared to **3** (EC_{50} 20 vs. 8.6 nM), but was much less efficient at recruiting β-arrestin-2 (EC_{50} 1423 vs. 166 nM). Thus, similarly to apelin, it appears that the C-terminal extremity of ELA is important for both binding and signaling. N-terminal mutated analogues **13**-**18**, which possess similar binding affinities compared to fragment **3**, also triggered $G\alpha_{i1}$ dissociation and β-arrestin-2 recruitment with similar potency, suggesting that the N-terminal fragment may not be crucial for activation of these pathways. This is

also similar to apelin, in which the N-terminal was found to be important for binding but had a marginal impact on signaling.[8,25] Altogether, these results suggest that the negative charge in the C-terminal Phe13 residue of **3** not only impacts binding affinity, but also alters functional properties of the APJ receptor**.**

Hypotensive effects of apelin-13, ELA and analogue 3

A growing body of literature demonstrates that apelin-13 possesses hypotensive effects in normal Sprague-Dawley and in spontaneously hypertensive rats.[22,23] Furthermore, the C-terminal Phe13 residue of apelin is central in this effect since its deletion or substitution by alanine reduces lowering of the mean arterial pressure (MAP).[22] Recently, Wang and coworkers reported that ELA relaxed pre-contracted mouse aortic rings.[32] However, the *in vivo* effects of ELA on blood pressure have not been determined. We thus investigated the impact of ELA and analogues **3** and **4** on blood pressure. Accordingly, apelin-13, ELA and its analogues **3** and **4** were administered to Sprague-Dawley rats by i.v. bolus (0.65 - 65 nmol/kg), then arterial blood pressure and heart rate were monitored via direct, continuous intra-carotid measurements (**Figure 3**). Apelin-13 rapidly lowered MAP in a dose-dependent manner, with a peak effect 30 seconds following administration. The maximal hypotensive effect of apelin-13, which corresponds to a 35 mmHg decrease in MAP, was observed at doses of 19.6 nmol/kg and 65 nmol/kg (**Figure 3A**). This first short-lasting depressor phase was followed by a hypertensive phase, returning to baseline approximately 100 seconds after apelin-13 injection. Finally, a compensatory mechanism led to a hypertensive phase that returned to baseline levels after 15 min. Administration of ELA in Sprague-Dawley rats

displayed a similar profile compared to that of apelin-13 up to 19.6 nmol/kg (**Figure 3B**). As observed with apelin-13, the blood pressure returned to baseline within 10-15 min after ELA injection. Determination of EC_{50} values by non-linear regression analysis revealed that ELA and apelin-13 have a similar *in vivo* potency at lowering blood pressure (6.14 ± 2.47 and 1.27 ± 1.04 nmol/kg, respectively). However, ELA had a different behavior compared to apelin-13 at the highest dose tested (65 nmol/kg), reaching the maximum average drop of -50 mmHg. Analogue **3**, when tested at doses of 6.5, 65 and 293 nmol/kg (**Figure 3C**), was less efficient in reducing MAP compared to ELA, which may be related to its lower efficacy to induce APJ internalization. Additionally, **3** did not induce a hypertensive rebound compared to apelin-13 and ELA, even at the highest dose tested. It should be noted that these analogues evoked small yet statistically significant increases in heart rates at the highest doses, an effect that is likely a compensatory mechanism to restore MAP (Supporting Information, Figure S3). Finally, compound **4** exhibited no hypotensive effect at 65 nmol/kg, and a marginal drop in MAP (-10 mmHg) at the highest dose of 650 nmol/kg (**Figure 3D**), consistent with its weaker potency to elicit APJ internalization. These observations are supported by previous work showing that the drop in MAP caused by C-terminally modified apelin peptides is related on their ability to recruit β-arrestin and induce APJ internalization.[21,22,28] They also underline the identification of **3** as a potent bioactive fragment of ELA. Furthermore, differences in the blood pressure profiles observed between apelin-13, ELA and **3** may tentatively be interpreted by the recruitment of distinct vasorelaxation mechanisms,[32] which remains to be explored.

Left ventricular developed pressure of apelin-13, ELA and analogue 3 in rat isolated-perfused heart

Apelin is known to be a potent inotropic agent.[12,13] In order to better understand the effect of ELA and analogue **3** on cardiac function, we performed *ex vivo* physiological experiments. Using the Langendorff perfused isolated rat heart, the effect of apelin-13, ELA and **3** on left ventricular developed pressure (LVDP) was assessed at concentrations ranging from 0.001 to 0.3 nM. (**Figure 4A-C**). EC_{50} values extrapolated from sigmoidal dose-response curves revealed that compound **3** was as potent as apelin-13 and ELA in inducing changes in LVDP (EC_{50} of 1.5 pM, 4.3 pM and 2.7 pM, respectively). Indeed, the three peptides induced a significant increase in LVDP, with a maximal effect at 0.03 nM. At this concentration, apelin-13 and ELA induced a strong LVDP effect (close to 200% above baseline) with a trend for ELA to be higher (**Figure 4D**). The efficacy of **3** to increase LVDP tended to be lower than the two endogenous ligands. However, statistical comparison between maximal effects obtained at 0.03 nM did not reveal any significant difference versus ELA or apelin-13 (**Figure 4D**).

Effects of apelin-13, ELA and analogue 3 on fluid homeostasis and left ventricular pressure

The effect of ELA on cardiac function and fluid homeostasis was next evaluated *in vivo*, with the help of echocardiography and metabolic assessment. In these experiments, compounds were delivered via i.v. infusion using osmotic minipumps at a constant flow rate of 36 pmol/g/min over 24 hours. *In vivo*, both apelin-13 and ELA produced a significant increase in fractional shortening, with a marginal impact on heart

rate, 6 and 24 h following i.v. administration (**Figure 5A-B**).[45] Although the inotropic effect of apelin-13 has been previously well documented,[46] these results demonstrate for the first time the inotropic effect of ELA. In the same experimental paradigm, the shorter fragment, compound **3**, tended to enhance left ventricular contractility, however without statistical significance compared to baseline.

In addition to their cardiovascular effects, apelin-13 and ELA are known to regulate fluid homeostasis, acting as aquaretic agents.[10,35] In this study, both apelin-13 and ELA increased daily urinary output in Sprague-Dawley Rats (**Figure 5C**). In contrast with its lower myocardial impact, **3** was as effective as the endogenous peptides to stimulate urine output (**Figure 5C**). There was no significant change in water intake (**Figure 5D**) or plasma volume (not shown) over the time period studied with any of the compounds. As expected,[35] i.v. injection of ELA and **3** induced a significant decrease in urine osmolality and electrolyte excretion (concentrations of Na^+ and K^+), compared to untreated rats (Supporting Information, Figure S4). These results are in agreement with recent studies demonstrating that administration of apelin-17 to lactating rats significantly induced an increase in diuresis that was accompanied by a reduction in urine osmolality.[9,10]

CONCLUSION

In conclusion, we report herein the first elucidation of the structure-activity relationship of ELA, a recently discovered endogenous ligand of the APJ receptor. The alanine scan led to an understanding of the structure-activity relationship of the peptide and to the discovery of analogue **3**, a significantly smaller bioactive fragment consisting of the last 14 amino acids of native ELA which binds APJ, activates $G\alpha_{i1}$ and β-arrestin-2

signaling pathways, and induces receptor internalization similarly to the parent peptide. The alanine scan revealed that the C-terminal moiety (Arg28, Val29, Pro30, Phe31, Pro32) and His26 residues are the most critical for binding and signaling. Additionally, replacements of N-terminal Arg20 and Arg21 only slightly decreased affinity. This SAR sharply contrasts with apelin-13, in which key pharmacophores (Arg2-Pro3-Arg4-Leu5) are mainly located at the N-terminal portion of the peptide. These differences suggest that both peptides may not bind exactly in the same way into the orthosteric binding site and pave the way toward the identification of additional residues of interest for interaction with APJ.

This study is also the first to characterize the cardiovascular effects of ELA and its fragment **3**. Indeed, as demonstrated by *ex vivo* isolated-perfused heart and *in vivo* blood pressure and echocardiographic measures, both ELA and **3** caused hypotensive effects and enhanced left ventricular contractility. Altogether, our results reveal that **3** represents a potent bioactive fragment of ELA and opens promising avenues for further exploitation of the therapeutic potential of ELA and the apelinergic system in cardiovascular diseases.

EXPERIMENTAL SECTION

Procedures for solid phase synthesis

Materials

Fmoc-protected (L)-amino acids were purchased from ChemImpex International (USA). 2-chlorotrityl chloride resin and [O-(7-azabenzotriazol-1-yl)-1,1,3,3-tetramethyluronium hexafluorophosphate] (HATU) were purchased from Matrix Innovation (Canada). All other reagents, purchased from Sigma-Aldrich (Canada), Fisher Scientific (USA) or ACP (Canada), were of the highest commercially available purity. All reagents and starting materials were used as received. Peptide synthesis was performed in 12 mL polypropylene cartridge with 20 μm PE frit from Applied Separations (USA).

Peptide synthesis

In a typical procedure, 2-chlorotrityl chloride resin (0.8 mmol/g, 0.1 g) was treated with Fmoc-protected amino acid (1 equiv.), *N,N*-diisopropylethylamine (DIPEA, 2 equiv.), in dichloromethane (DCM, 4 mL). The mixture was shaken for 2 h on an orbital shaker at room temperature, then the resin was sequentially washed for 3-min periods with DCM (2x 5 mL), 2-propanol (1x 5 mL), DCM (1x 5 mL), 2-propanol (1x 5 mL), DCM (2x 5 mL). A capping solution of DCM/MeOH/DIPEA (7/2/1, 5 mL) was then added and the mixture shaken for 1 h at room temperature and washed with the above solvent sequence. The Fmoc group was then deprotected with 20% piperidine/DMF (*N,N*-dimethylformamide) during 15 min, then the subsequent Fmoc-protected amino acid (5 equiv.) was attached in the presence of HATU (5 equiv.), DIPEA (10 equiv.) in DMF (4

mL). This reaction proceeded for 30 min, unless the amino acid was being added to a Pro residue, in which case reaction lasted for 60 min. Then piperidine (20% in DMF) was used to deprotect the Fmoc group at every step. The resin was washed after each coupling step and deprotected with the above sequence of solvents. Peptides were cleaved from the resin with a mixture of TFA (trifluoroacetic acid)/H_2O/TIPS (triisopropylsilane)/EDT (1,2-ethandithiol), 37/1/1/1, v/v (4 mL / 0.1 g of resin) for 4 h at room temperature. When needed, disulfide bridge between cysteines was formed using a solution of I_2/MeOH (10% w/v) (dropwise addition until persistent yellow color), after dissolution of the lyophilized crude in a 70% aqueous acetic acid solution (1 mg/mL). After 15 min stirring, the crude was lyophilized again, then precipitated in *tert*-butyl methyl ether (TBME) at 0°C. Non-cyclized analogues were directly precipitated in TBME. The suspension was centrifuged, the supernatant removed and the crude product re-dissolved in water. Purification by reverse-phase HPLC yielded the desire products, isolated as white powders after lyophilization.

Peptide purification and characterization

Crude peptides were purified by reverse-phase chromatography using a preparative HPLC from Waters (Autosampler 2707, Quaternary gradient module 2535, UV detector 2489, fraction collector WFCIII) equipped with an ACE5 C_{18} column (250 x 21.2 mm, 5 µm spherical particle size) and water + 0.1% TFA and acetonitrile as eluents. To determine purity, analytical UPLC chromatograms were recorded on a Waters Acquity H Class equipped with an Acquity UPLC BEH C_{18} column (1.7 µm particles size, 2.1 x 50 mm) using the following gradient: water + 0.1% TFA and acetonitrile (0→0.2 min: 5%

acetonitrile; 0.2→1.5 min: 5%→95%; 1.5→1.8 min: 95%; 1.8→2.0 min: 95%→5%; 2.0→2.5 min: 5%). All analogues possessed UV purity >95% (except for **9**, **12** and **14** possessing purity >93%) and molecular weights were determined by mass spectrometry (Electrospray infusion ESI-Q-Tof from Maxis) and High Resolution Mass Spectroscopy (HRMS).

Binding affinity and plasma stability

Materials

High glucose Dulbecco's Modified Eagle Medium (DMEM), G418 and penicillin/ streptomycin were purchased from Invitrogen Life Technologies (Canada). Fetal bovine serum (FBS) was purchased from Wisent (Canada) and bovine serum albumin (BSA) from BioShop (Canada). White opaque 96-well half area plates were purchased from PerkinElmer (Canada). Polyethylenimine (branched PEI) was obtained from Polysciences (USA). Coelenterazine-400A (DeepBlueC) was purchased from Biosynth International Inc. (USA). $BRET^2$ measurements were performed on a GeniosPro plate reader from Tecan (USA). Apelin-13[Glp^{65}, Nle^{75}, Tyr^{77}][^{125}I] (specific activity 820 Ci/mmol) was prepared using IODO-GEN (1,3,4,6-tetrachloro-3a, 6a-diphenyl-glycoluril; Thermo Scientific Pierce, Canada) as described by Fraker and Speck.[47] Briefly, 10 µL of a 1 mM peptide solution was incubated with 20 µg of IODO-GEN, 80 µL of 100 mM borate buffer (pH 8.5), and 1 mCi of Na-^{125}I for 30 min at room temperature, and was then purified by reversed-phase HPLC on a C_{18} column. The specific radioactivity of the labeled peptide was determined by self-displacement and saturation-binding analysis.

Cell culture

Stably transfected HEK293 cells expressing the YFP epitope-tagged human APJ were cultured in high glucose DMEM supplemented with 10% FBS. Cells were kept in a humidified atmosphere with 5% CO_2 at 37°C according to the manufacturer's instructions. G418 and penicillin/streptomycin were used as selection agent and antibiotics, respectively.

Radioligand binding

HEK293 cells expressing the YFP epitope-tagged human APJ were washed once with PBS and subjected to one freeze-thaw cycle. Broken cells were then gently scraped in resuspension buffer (1 mM EDTA and 10 mM Tris-HCl, pH 7.5), centrifuged at 3500 g for 15 min at 4°C and resuspended in binding buffer (50 mM Tris-HCl buffer, pH 7.5, containing 0.2% BSA). Competitive radioligand binding experiments were performed by incubating cell membranes (15 μg) with 0.2 nM Apelin-13[Glp^{65}, Nle^{75}, Tyr^{77}][^{125}I] (820 Ci/mmol) and increasing concentrations of various analogues (10^{-11} to 10^{-5} M) for 1 h at room temperature in a final volume of 200 μL. Bound radioactivity was separated from free ligand by filtration through GF/C glass fiber filter plates (Millipore, Billerica, MA) pre-soaked for 1 h in PEI 0.2% at 4°C and washed 3 times with 170 μL of ice-cold washing buffer (50 mM Tris-HCl buffer, pH 7.5, 0.2% BSA). Receptor-bound radioactivity was counted in a γ-counter 1470 Wizard form PerkinElmer (80% counting efficiency). Nonspecific binding was measured in the presence of 10^{-5} M unlabeled apelin-13 and represented less than 5% of total binding. K_i values were determined from dose-response curves as the unlabeled ligand concentration inhibiting 50% of [^{125}I]-

apelin-13 specific binding and using the Cheng-Prusoff equation.[48] All binding data were calculated and plotted using GraphPad Prism 6 and represent the mean ± SEM of three determinations.

Plasma Stability

27 µL of rat plasma (obtained from rat blood by keeping the translucent phase after centrifugation at 13000 rpm during 5 min at 4°C) and 6 µL of a 1 mM aqueous solution of ELA were incubated at 37°C for 2, 5 and 10 min. The proteolytic degradation was stopped by adding 70 µL of a 10% aqueous solution of trichloroacetic acid (TCA). After vortexing and centrifugation at 13000 rpm for 20 min at 4°C, the supernatant was filtered on a 4 mm nylon 0.2 µm syringe filter and analyzed by HPLC-MS (Waters 2695 with ACE C_{18} column 2.0 x 100 mm, 2.7 µm spherical particle size and Electrospray micromass ZQ-2000 from Waters).

$G\alpha_{i1}$ activation, β-arrestin-2 recruitment and internalization assays

Cell culture and transfections

HEK293 cells were allowed to grow in high glucose DMEM supplemented with 10% FBS, 100 U/mL penicillin/streptomycin, 2 mM glutamine, and 20 mM HEPES at 37˚C in a humidified chamber at 5% CO_2. All transfections were carried out with branched PEI as previously described.[49]

G-Protein activation and β-arrestin-2 recruitment

HEK293 cells were seeded in T175 flasks. After 24h, cells were transfected with the previously described plasmids coding for hAPJ, $G\alpha_{i1}$-RlucII(91),[40] GFP10-$G\gamma_2$,[40] and $G\beta_1$ (from cDNA.org) or for hAPJ-GFP10[25] and RlucII-β-arrestin-2.[39]

BRET experiments

Cells were seeded into white 96 well plates (BD Falcon) at a concentration of 50000 cells/well 24 h after transfection and incubated at 37˚C overnight. Cells were then washed with PBS and 90 µL of HBSS was added in each well. Then, cells were stimulated with analogues at concentrations ranging from 10^{-5} M to 10^{-11} M for 5 min at 37˚C ($G\alpha_{i1}$) or for 30 min at room temperature (β-arrestin-2). After stimulation, 5 µM of coelanterazine 400A was added to each well and the plate was read using the $BRET^2$ filter set of a GeniosPro plate reader (Tecan, Austria). The $BRET^2$ ratio was determined as $GFP10_{em}/RlucII_{em}$. Data were plotted and EC_{50} values were determined using GraphPad Prism 6. Each data point represents the mean ± SEM of at least three different experiments each done in triplicate.

Assessment of internalization by Enzyme-Linked Immunosorbent Assay (ELISA)

HEK293 cells were seeded in 24-well plates precoated with 0.1 mg/mL poly-L-Lysine (sigma) at 170 000 cells/well. 48 h post-transfection with the human HA-tagged APJ receptor, cells were washed and stimulated with compounds at concentrations ranging from 10^{-6} M to 10^{-11} M for 30 min at 37˚C in HBSS. Cells were then fixed in 3.7% (v/v) formaldehyde/Tris-buffered saline (TBS) (20 mM Tris-HCl, pH 7.5 and 150 mM NaCl) for 5 min at room temperature. Cells were then washed twice with TBS and incubated 30

min with TBS containing 1% BSA at room temperature to block non-specific binding. A monoclonal anti-HA-peroxidase antibody (clone 3F10, Roche Applied Sciences) was then added at a dilution of 1:1000 in TBS-BSA 1% for 60 min. Following the incubation with the primary antibody, cells were washed twice with TBS and 250 µL of 3,3′,5,5′-tetramethylbenzidine (Sigma-Aldrich, Canada) were added. The plates were incubated at room temperature and the reaction was stopped using 250 µL of HCl 2N. 200 µL of the colorimetric reaction was transferred to a 96-well plate and the absorbance was measured at 450 nm. Cells transfected with empty vector (pEYFPC1 modified where we replaced the YFP by two HA) were used to determine background. Data were plotted and EC_{50} values were determined by using GraphPad Prism 6. Each data point represents the mean ± SEM of at least three different experiments. The optical density (DO) measured at 1 µM for ELA, **3** or **4** was normalized to the DO measured at 1 µM for apelin-13 providing the percentage of internalization induced by these compounds versus apelin-13, set at 100% as the reference.

Cardiovascular assays

Animals

Adult male Sprague Dawley rats (Charles River Laboratories, St-Constant, Quebec, Canada) were maintained on a 12 h light/12 h dark cycle with access to food and water *ad libitum*. The animal experimental procedures in this study were approved by the Animal Care Committee of Université de Sherbrooke and were in accordance with policies and directives of the Canadian Council on Animal Care.

Hypotensive effects

Rats were anaesthetized with a mixture of ketamine/xylaxine (87 mg/kg: 13 mg/kg, i.m.) and placed in supine position on a heating pad. Mean, systolic, and diastolic arterial blood pressure, as well as heart rate, were measured through a catheter (PE 50 filled with heparinized saline) inserted in the right carotid artery and connected to a Micro-Med transducer (model TDX-300, USA) linked to a blood pressure Micro-Med analyzer (model BPA-100c). Another catheter was inserted in the left jugular vein for bolus injections (1 mL/kg, 5-10 s) of vehicle (isotonic saline), or compounds at different doses 0.65, 1.96, 6.5, 19.6, 65 and 293 nmol/kg. Rats were given vehicle first, then only one dose of a single analogue prior to euthanasia. For relative potency evaluation, changes in blood pressure from baseline to maximal effect post-injection in individual animals were determined. Data represents mean ± SEM of at least six different experiments.

Isolated-perfused heart

Sprague-Dawley rats were anaesthetized with isoflurane then hearts were excised and immediately mounted, via the ascending aorta, into a Langendorff apparatus and perfused with aerated tyrode's solution. Mechanical activity was monitored by the careful insertion of a saline-filled latex balloon into the left ventricle. Left ventricular pressure was continuously monitored through a pre-calibrated physiological pressure transducer (Molecular Devices, Sunnyvale, CA). Data recording started only once variables were stable (10 min), after which a baseline was defined. Then, increasing concentrations of compounds were perfused at 0.001, 0.003, 0.01, 0.03, 0.1 and 0.3 nM. A 5-min washout period was performed between each concentration. Data for left ventricular developed pressure (LVDP) were collected and processed using the Clampfit 10.2 program

(Molecular Devices). Data represents the mean ± SEM of at least five different experiments.

Surgical procedure for continuous analogues administration using osmotic minipumps

A PE-50 catheter dedicated to compounds infusions was inserted into the right jugular vein and tunnelled subcutaneously upon the dorsal neck, then secured open by a heparin-lock while rats were allowed to recover for 24 hours. Then, the right jugular vein was connected to an osmotic minipumps (Alzet® osmotic pumps, model 2001D, Cupertino, CA) implanted at the dorsal neck site in isoflurane-anaesthetized rats. The rate of delivery was 36 pmol/g/min.

Echocardiography

Transthoracic echocardiography was performed in isoflurane-anaesthetized closed-chest Sprague-Dawley rats (2%; 1.5 mL/min; Baxter), prior and 6-24 hours after surgical procedures (each animal being is own control) using a s12 HP 5-12 mHz high resolution small footprint transducer at an acquisition rate of 60 Hz (Hewlett-Packard, Sonos 5500). A two-dimensional short axis view of the LV was obtained at the level of the papillary muscle, and the M-mode tracing was recorded. From these recordings, LV Diastolic and Systolic Diameters (LVDD; LVSD) as well as LV diastolic and systolic wall thickness were measured by the leading edge method according to the American Society of Echocardiography guidelines. Fractional Shortening (FS) was established by the formula: ([LVEDd-LVESd/LVEDd] x 100%). Data represents the mean ± SEM of at least five different experiments.

Fluid homeostasis

Rats were kept inside metabolic cages during 24 h to collect and measure urine output and water intake. Plasma volumes were measured at the end of the experiment with use of fluorescent-labeled albumin molecules.[50]

Urine Osmolality

Measurements of urine osmolality and determination of Na^+ and K^+ ion concentrations in urine were performed at the biochemical department of the Centre Hospitalier Universitaire de Sherbrooke (CHUS) and were determined by a Vitros 750 XRC analyser (Johnson-Johnson Clinical Diagnostics; Rochester, NY).

Statistical analyses

In the Langendorff assay, differences between the different doses tested and the isolated-perfused heart treated with saline were determined using one-way ANOVA followed by Bonferroni's test. In the *in vivo* studies, a two-way ANOVA followed by Bonferroni test was performed to compare the impact of each compound on the heart rate evolution during 24 hours. For multi-group comparisons, a one-way ANOVA followed by Bonferroni's test was used. $p < 0.05$ was considered statistically significant.

ACKNOWLEDGMENTS

Financial support from Université de Sherbrooke, the Natural Sciences and Engineering Research Council of Canada, the Canada Foundation for Innovation, Merck Sharpe & Dohme (donation to the Faculty of Medicine and Health Sciences of Université de Sherbrooke) and the FRQS-funded Réseau Québécois de Recherche sur le Médicament (RQRM) is acknowledged. The Institut de Pharmacologie de Sherbrooke (IPS) and MITACS are also acknowledged for scholarship grants to A.M and X.S. M.A.-M. is the recipient of a Heart and Stroke Foundation of Canada (HFSC) New Investigator award. P.S. is the recipient of the Canada Research Chair in Neurophysiopharmacology of Chronic Pain. E.M. is a member of the FRQNT-funded Proteo Network. The authors would also thank Prof. Michel Bouvier (Institut de Recherche en Immunologie et Cancer, Montréal, Québec, Canada) for the use of human $G\alpha_{i1}$ and β-arrestin-2 biosensors.

SUPPORTING INFORMATION

Analytical Ultrahigh performance liquid chromatography-Mass spectrometry (UPLC-MS) and High Resolution Mass Spectrometry (HRMS) spectra of the different compounds described in this manuscript, plasma stability, changes in heart rates and urine osmolality are presented in the supporting information. This material is available free of charge via the Internet at http://pubs.acs.org.

AUTHOR INFORMATION

Corresponding Author

* Prof. Éric Marsault

Phone: +1 819.821.8000 ext 72433

Fax: +1 819.564.5400

Email: eric.marsault@usherbrooke.ca

Author Contributions

$ E.M. and P.S. contributed equally to directing this study.

Notes

The authors declare no competing financial interest.

ABBREVIATIONS USED

bpm: beats per minute, BRET: Bioluminescence Resonance Energy Transfer, cAMP: cyclic Adenosine Monophosphate, DCM: dichloromethane, DIAD: diisopropylazodicarboxylate, DIPEA: *N,N*-diisopropylethylamine, DMF: *N,N*-dimethylformamide, EDT: 1,2-ethandithiol, ELISA: Enzyme-Linked Immunosorbent Assay, ERK1/2: Extracellular Signal-Regulated Kinases 1/2, FRET: Förster Resonance Energy Transfer, GPCR: G Protein-Coupled Receptor, HATU: O-(7-azabenzotriazol-1-yl)-1,1,3,3-tetramethyluronium hexafluorophosphate, HEK: Human Embryonic Kidney, HPLC: High Performance Liquid Chromatography, HRMS: High Resolution Mass Spectrometry, LVDP: Left Ventricular Developed Pressure, MAP: Mean Arterial Pressure, SAR: Structure-Activity Relationship, TBME: *tert*-butyl methyl ether, TFA: Trifluoroacetic acid, TIPS: Triisopropylsilane.

REFERENCES

(1) O'Dowd, B. F.; Heiber, M.; Chan, A.; Heng, H. H.; Tsui, L. C.; Kennedy, J. L.; Shi, X.; Petronis, A.; George, S. R.; Nguyen, T. A Human Gene That Shows Identity with the Gene Encoding the Angiotensin Receptor Is Located on Chromosome 11. *Gene* **1993**, *136*, 355–360.

(2) Tatemoto, K.; Hosoya, M.; Habata, Y.; Fujii, R.; Kakegawa, T.; Zou, M. X.; Kawamata, Y.; Fukusumi, S.; Hinuma, S.; Kitada, C.; Kurokawa, T.; Onda, H.; Fujino, M. Isolation and Characterization of a Novel Endogenous Peptide Ligand for the Human APJ Receptor. *Biochem. Biophys. Res. Commun.* **1998**, *251*, 471–476.

(3) O'Carroll, A.-M.; Lolait, S. J.; Harris, L. E.; Pope, G. R. The Apelin Receptor APJ: Journey from an Orphan to a Multifaceted Regulator of Homeostasis. *J. Endocrinol.* **2013**, *219*, R13–R35.

(4) Zhen, E. Y.; Higgs, R. E.; Gutierrez, J. a. Pyroglutamyl Apelin-13 Identified as the Major Apelin Isoform in Human Plasma. *Anal. Biochem.* **2013**, *442*, 1–9.

(5) O'Carroll, A. M.; Selby, T. L.; Palkovits, M.; Lolait, S. J. Distribution of mRNA Encoding B78/apj, the Rat Homologue of the Human APJ Receptor, and Its Endogenous Ligand Apelin in Brain and Peripheral Tissues. *Biochim. Biophys. Acta - Gene Struct. Expr.* **2000**, *1492*, 72–80.

(6) Hosoya, M.; Kawamata, Y.; Fukusumi, S.; Fujii, R.; Habata, Y.; Hinumat, S.; Kitada, C.; Honda, S.; Kurokawa, T.; Onda, H.; Nishimura, O.; Fujino, M. Molecular and Functional Characteristics of APJ: Tissue Distribution of mRNA and Interaction with the Endogenous Ligand Apelin. *J. Biol. Chem.* **2000**, *275*, 21061–21067.

(7) Lee, D. L.; Cheng, R.; Nguyen, T.; Fan, T.; Kariyawasam, A. P.; Liu, Y.; Osmond, D. H.; George, S. R.; O'Dowd, B. F. Characterization of Apelin, the Ligand for the APJ Receptor. *J. Neurochem.* **2000**, *74*, 34–41.

(8) Medhurst, A. D.; Jennings, C. a.; Robbins, M. J.; Davis, R. P.; Ellis, C.; Winborn, K. Y.; Lawrie, K. W. M.; Hervieu, G.; Riley, G.; Bolaky, J. E.; Herrity, N. C.; Murdock, P.; Darker, J. G. Pharmacological and Immunohistochemical Characterization of the APJ Receptor and Its Endogenous Ligand Apelin. *J. Neurochem.* **2003**, *84*, 1162–1172.

(9) Hus-Citharel, A.; Bodineau, L.; Frugière, A.; Joubert, F.; Bouby, N.; Llorens-Cortes, C. Apelin Counteracts Vasopressin-Induced Water Reabsorption via Cross Talk between Apelin and Vasopressin Receptor Signaling Pathways in the Rat Collecting Duct. *Endocrinology* **2014**, *155*, 4483–4493.

(10) De Mota, N.; Reaux-Le Goazigo, A.; El Messari, S.; Chartrel, N.; Roesch, D.; Dujardin, C.; Kordon, C.; Vaudry, H.; Moos, F.; Llorens-Cortes, C. Apelin, a Potent Diuretic Neuropeptide Counteracting Vasopressin Actions through Inhibition of Vasopressin Neuron Activity and Vasopressin Release. *Proc. Natl.*

Acad. Sci. U. S. A. **2004**, *101*, 10464–10469.

(11) Brame, A. L.; Maguire, J. J.; Yang, P.; Dyson, A.; Torella, R.; Cheriyan, J.; Singer, M.; Glen, R. C.; Wilkinson, I. B.; Davenport, A. P. Design, Characterization, and First-in-Human Study of the Vascular Actions of a Novel Biased Apelin Receptor Agonist. *Hypertension* **2015**, *65*, 834–840.

(12) Narayanan, S.; Harris, D. L.; Maitra, R.; Runyon, S. P. Regulation of the Apelinergic System and Its Potential in Cardiovascular Disease: Peptides and Small Molecules as Tools for Discovery. *J. Med. Chem.* **2015**, *58*, 7913–7927.

(13) Dalzell, J. R.; Rocchiccioli, J. P.; Weir, R. A. P.; Jackson, C. E.; Padmanabhan, N.; Gardner, R. S.; Petrie, M. C.; McMurray, J. J. V. The Emerging Potential of the Apelin-APJ System in Heart Failure. *J. Card. Fail.* **2015**, *21*, 489–498.

(14) Bertrand, C.; Valet, P.; Castan-Laurell, I. Apelin and Energy Metabolism. *Front. Physiol.* **2015**, *6*, 115-119.

(15) Chaves-Almagro, C.; Castan-Laurell, I.; Dray, C.; Knauf, C.; Valet, P.; Masri, B. Apelin Receptors: From Signaling to Antidiabetic Strategy. *Eur. J. Pharmacol.* **2015**, *763*, 1–11.

(16) Tatemoto, K.; Takayama, K.; Zou, M. X.; Kumaki, I.; Zhang, W.; Kumano, K.; Fujimiya, M. The Novel Peptide Apelin Lowers Blood Pressure via a Nitric Oxide-Dependent Mechanism. *Regul. Pept.* **2001**, *99*, 87–92.

(17) Hamada, J.; Kimura, J.; Ishida, J.; Kohda, T.; Morishita, S.; Ichihara, S.; Fukamizu, A. Evaluation of Novel Cyclic Analogues of Apelin. *Int. J. Mol. Med.* **2008**, *22*, 547–552.

(18) D'Aniello, C.; Lonardo, E.; Iaconis, S.; Guardiola, O.; Liguoro, A. M.; Liguori, G. L.; Autiero, M.; Carmeliet, P.; Minchiotti, G. G Protein-Coupled Receptor APJ and Its Ligand Apelin Act Downstream of Cripto to Specify Embryonic Stem Cells toward the Cardiac Lineage through Extracellular Signal-Regulated kinase/p70S6 Kinase Signaling Pathway. *Circ. Res.* **2009**, *105*, 231–238.

(19) Yue, P.; Jin, H.; Xu, S.; Aillaud, M.; Deng, A. C.; Azuma, J.; Kundu, R. K.; Reaven, G. M.; Quertermous, T.; Tsao, P. S. Apelin Decreases Lipolysis via G(q), G(i), and AMPK-Dependent Mechanisms. *Endocrinology* **2011**, *152*, 59–68.

(20) Lee, D. K.; Ferguson, S. S. G.; George, S. R.; O'Dowd, B. F. The Fate of the Internalized Apelin Receptor Is Determined by Different Isoforms of Apelin Mediating Differential Interaction with Beta-Arrestin. *Biochem. Biophys. Res. Commun.* **2010**, *395*, 185–189.

(21) El Messari, S.; Iturrioz, X.; Fassot, C.; De Mota, N.; Roesch, D.; Llorens-Cortes, C. Functional Dissociation of Apelin Receptor Signaling and Endocytosis: Implications for the Effects of Apelin on Arterial Blood Pressure. *J. Neurochem.* **2004**, *90*, 1290–1301.

(22) Lee, D. K.; Saldivia, V. R.; Nguyen, T.; Cheng, R.; George, S. R.; O'Dowd, B. F. Modification of the Terminal Residue of Apelin-13 Antagonizes Its Hypotensive

Action. *Endocrinology* **2005**, *146*, 231–236.

(23) Murza, A.; Besserer-Offroy, É.; Côté, J.; Bérubé, P.; Longpré, J.-M.; Dumaine, R.; Lesur, O.; Auger-Messier, M.; Leduc, R.; Sarret, P.; Marsault, É. C-Terminal Modifications of Apelin-13 Significantly Change Ligand Binding, Receptor Signaling, and Hypotensive Action. *J. Med. Chem.* **2015**, *58*, 2431–2440.

(24) Vickers, C.; Hales, P.; Kaushik, V.; Dick, L.; Gavin, J.; Tang, J.; Godbout, K.; Parsons, T.; Baronas, E.; Hsieh, F.; Acton, S.; Patane, M.; Nichols, A.; Tummino, P. Hydrolysis of Biological Peptides by Human Angiotensin-Converting Enzyme-Related Carboxypeptidase. *J. Biol. Chem.* **2002**, *277*, 14838–14843.

(25) Murza, A.; Parent, A.; Besserer-Offroy, E.; Tremblay, H.; Karadereye, F.; Beaudet, N.; Leduc, R.; Sarret, P.; Marsault, É. Elucidation of the Structure-Activity Relationships of Apelin: Influence of Unnatural Amino Acids on Binding, Signaling, and Plasma Stability. *ChemMedChem* **2012**, *7*, 318–325.

(26) Murza, A.; Belleville, K.; Longpré, J.-M.; Sarret, P.; Marsault, E. Stability and Degradation Patterns of Chemically Modified Analogs of Apelin-13 in Plasma and Cerebrospinal Fluid. *Biopolymers* **2014**, *102*, 297–303.

(27) Iturrioz, X.; Gerbier, R.; Leroux, V.; Alvear-Perez, R.; Maigret, B.; Llorens-Cortes, C. By Interacting with the C-Terminal Phe of Apelin, Phe255 and Trp259 in Helix VI of the Apelin Receptor Are Critical for Internalization. *J. Biol. Chem.* **2010**, *285*, 32627–32637.

(28) Ceraudo, E.; Galanth, C.; Carpentier, E.; Banegas-Font, I.; Schonegge, A.-M.; Alvear-Perez, R.; Iturrioz, X.; Bouvier, M.; Llorens-Cortes, C. Biased Signaling Favoring Gi over β-Arrestin Promoted by an Apelin Fragment Lacking the C-Terminal Phenylalanine. *J. Biol. Chem.* **2014**, *289*, 24599–24610.

(29) Chng, S. C.; Ho, L.; Tian, J.; Reversade, B. ELABELA: A Hormone Essential for Heart Development Signals via the Apelin Receptor. *Dev. Cell* **2013**, *27*, 672–680.

(30) Pauli, A.; Norris, M. L.; Valen, E.; Chew, G.-L.; Gagnon, J. a; Zimmerman, S.; Mitchell, A.; Ma, J.; Dubrulle, J.; Reyon, D.; Tsai, S. Q.; Joung, J. K.; Saghatelian, A.; Schier, A. F. Toddler: An Embryonic Signal That Promotes Cell Movement via Apelin Receptors. *Science* **2014**, *343*, 1–13.

(31) Pauli, A.; Valen, E.; Schier, A. F. Identifying (non-)coding RNAs and Small Peptides: Challenges and Opportunities. *Bioessays* **2015**, *37*, 103–112.

(32) Wang, Z.; Yu, D.; Wang, M.; Wang, Q.; Kouznetsova, J.; Yang, R.; Qian, K.; Wu, W.; Shuldiner, A.; Sztalryd, C.; Zou, M.; Zheng, W.; Gong, D.-W. Elabela-Apelin Receptor Signaling Pathway Is Functional in Mammalian Systems. *Sci. Rep.* **2015**, *5*, 8170.

(33) Reichman-Fried, M.; Raz, E. Small Proteins, Big Roles: The Signaling Protein Apela Extends the Complexity of Developmental Pathways in the Early Zebrafish Embryo. *BioEssays* **2014**, *36*, 741–745.

(34) Helker, C. S.; Schuermann, A.; Pollmann, C.; Chng, S. C.; Kiefer, F.; Reversade,

B.; Herzog, W. The Hormonal Peptide Elabela Guides Angioblasts to the Midline during Vasculogenesis. *Elife* **2015**, *4*, 1–13.

(35) Deng, C.; Chen, H.; Yang, N.; Feng, Y.; Hsueh, A. J. W. Apela Regulates Fluid Homeostasis by Binding to the APJ Receptor to Activate Gi Signaling. *J. Biol. Chem.* **2015**, *290*, 18261–18268.

(36) Ho, L.; Tan, S. Y. X.; Wee, S.; Wu, Y.; Tan, S. J. C.; Ramakrishna, N. B.; Chng, S. C.; Nama, S.; Sczerbinska, I.; Chan, Y.-S.; Avery, S.; Tsuneyoshi, N.; Ng, H. H.; Gunaratne, J.; Dunn, N. R.; Reversade, B. ELABELA Is an Endogenous Growth Factor That Sustains hESC Self-Renewal via the PI3K/AKT Pathway. *Cell Stem Cell* **2015**, *17*, 435–447.

(37) Langelaan, D. N.; Reddy, T.; Banks, A. W.; Dellaire, G.; Dupré, D. J.; Rainey, J. K. Structural Features of the Apelin Receptor N-Terminal Tail and First Transmembrane Segment Implicated in Ligand Binding and Receptor Trafficking. *Biochim. Biophys. Acta* **2013**, *1828*, 1471–1483.

(38) Bowers, R. R.; Festuccia, W. T. L.; Song, C. K.; Shi, H.; Migliorini, R. H.; Bartness, T. J. Sympathetic Innervation of White Adipose Tissue and Its Regulation of Fat Cell Number. *Am. J. Physiol. Regul. Integr. Comp. Physiol.* **2004**, *286*, R1167–R1175.

(39) Zimmerman, B.; Beautrait, A.; Aguila, B.; Charles, R.; Escher, E.; Claing, A.; Bouvier, M.; Laporte, S. A. Differential β-Arrestin-Dependent Conformational Signaling and Cellular Responses Revealed by Angiotensin Analogs. *Sci. Signal.* **2012**, *5*, ra33.

(40) Galés, C.; Van Durm, J. J. J.; Schaak, S.; Pontier, S.; Percherancier, Y.; Audet, M.; Paris, H.; Bouvier, M. Probing the Activation-Promoted Structural Rearrangements in Preassembled Receptor-G Protein Complexes. *Nat. Struct. Mol. Biol.* **2006**, *13*, 778–786.

(41) Pace, C. N.; Scholtz, J. M. A Helix Propensity Scale Based on Experimental Studies of Peptides and Proteins. *Biophys. J.* **1998**, *75*, 422–427.

(42) Langelaan, D. N.; Bebbington, E. M.; Reddy, T.; Rainey, J. K. Structural Insight into G-Protein Coupled Receptor Binding by Apelin. *Biochemistry* **2009**, *48*, 537–548.

(43) Macaluso, N. J. M.; Glen, R. C. Exploring the "RPRL" Motif of Apelin-13 through Molecular Simulation and Biological Evaluation of Cyclic Peptide Analogues. *ChemMedChem* **2010**, *5*, 1247–1253.

(44) Vogt, W. Oxidation of Methionyl Residues in Proteins: Tools, Targets, and Reversal. *Free Radic. Biol. Med.* **1995**, *18*, 93–105.

(45) Lesur, O.; Chagnon, F.; Murza, A.; Sarret, P.; Marsault, E.; Salvail, D. Apelin Is Cardioprotective and Life-Saving Over Dobutamine in a Murine Model of Endotoxin-Induced Myocardial Dysfunction. *Intensive Care Medicine Experimental* **2014**, *2(Suppl 1)*, 11.

(46) Szokodi, I.; Tavi, P.; Földes, G.; Voutilainen-Myllylä, S.; Ilves, M.; Tokola, H.; Pikkarainen, S.; Piuhola, J.; Rysä, J.; Tóth, M.; Ruskoaho, H. Apelin, the Novel Endogenous Ligand of the Orphan Receptor APJ, Regulates Cardiac Contractility. *Circ. Res.* **2002**, *91*, 434–440.

(47) Fraker, P. J.; Speck, J. C. Protein and Cell Membrane Iodinations with a Sparingly Soluble Chloroamide, 1,3,4,6-Tetrachloro-3a,6a-Diphrenylglycoluril. *Biochem. Biophys. Res. Commun.* **1978**, *80*, 849–857.

(48) Cheng, Y.; Prusoff, W. H. Relationship between the Inhibition Constant (K1) and the Concentration of Inhibitor Which Causes 50 per Cent Inhibition (I50) of an Enzymatic Reaction. *Biochem. Pharmacol.* **1973**, *22*, 3099–3108.

(49) Ehrhardt, C.; Schmolke, M.; Matzke, A.; Knoblauch, A.; Will, C.; Wixler, V.; Ludwig, S. Polyethylenimine, a Cost-Effective Transfection Reagent. *Signal Transduct.* **2006**, *6*, 179–184.

(50) Gillen, C. M.; Takamata, a; Mack, G. W.; Nadel, E. R. Measurement of Plasma Volume in Rats with Use of Fluorescent-Labeled Albumin Molecules. *J. Appl. Physiol.* **1994**, *76*, 485–489.

Figure 1

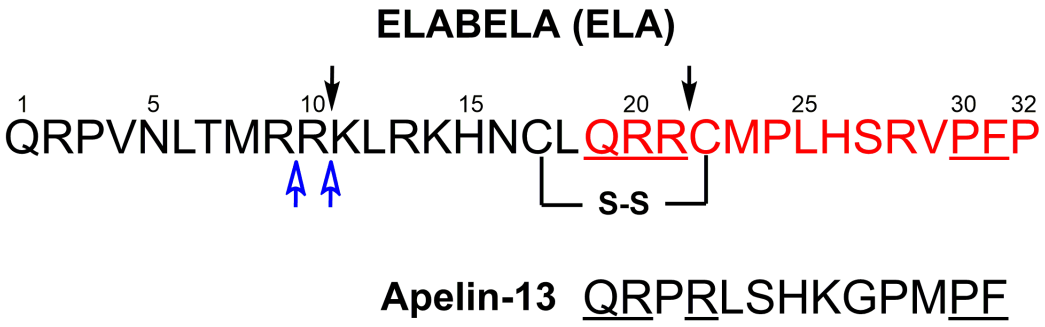

Figure 1. Structure of ELA and apelin-13. Black arrows indicate predicted convertase cleavage sites[29] and blue arrows denote cleavages observed after incubation in rat plasma. The potent bioactive fragment **3** (ELA(19-32)), in red, was identified by comparison of the structural similarities between ELA and the main pharmacophores of apelin-13 (common amino acids underlined).

Figure 2

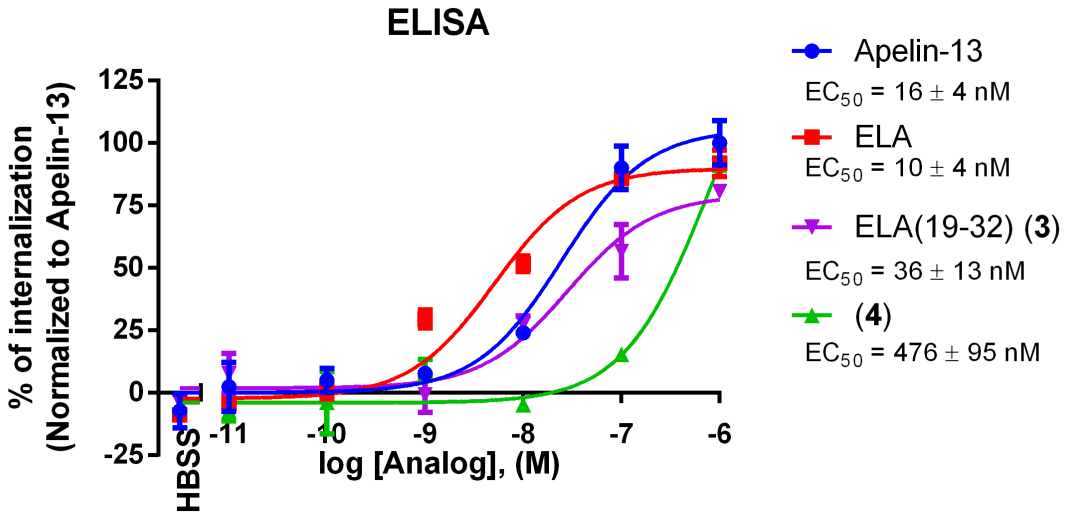

Figure 2. APJ receptor internalization as a function of concentration of apelin-13, ELA, **3** and **4**. Cell surface expression was measured at concentrations ranging from 10^{-6} M to 10^{-11} M by enzyme-linked immunosorbent assay in HEK293 cells transiently expressing the HA-hAPJ receptor. Values represent the mean ± SEM of at least three determinations.

Figure 3

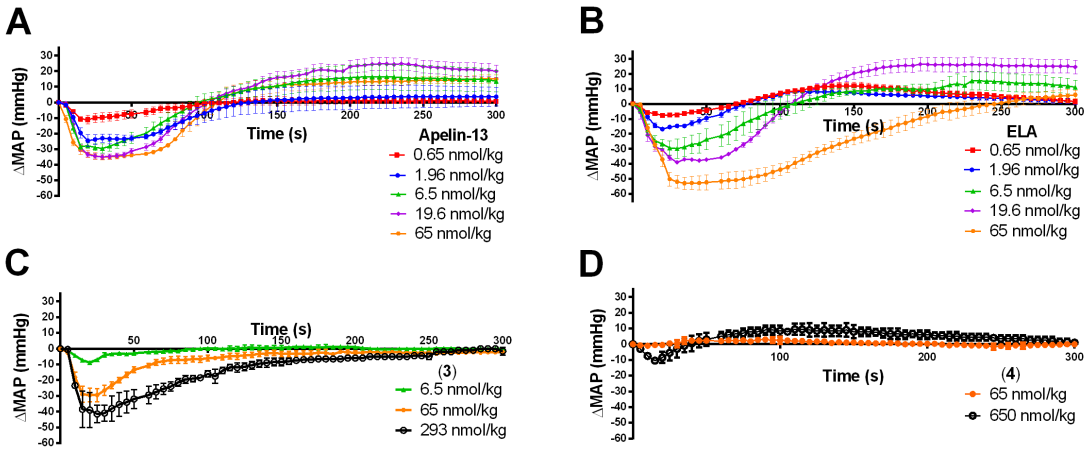

Figure 3. Effects of apelin-13, ELA, **3** and **4** on mean arterial pressure (ΔMAP) in anaesthetized rats. Tracings depicting the hypotensive effects of (**A**) apelin-13, (**B**) ELA, (**C**) **3** and (**D**) **4** in rats after administration of increasing doses of each compound. Each bar represents the average value ± S.E.M obtained with 6-8 animals.

Figure 4

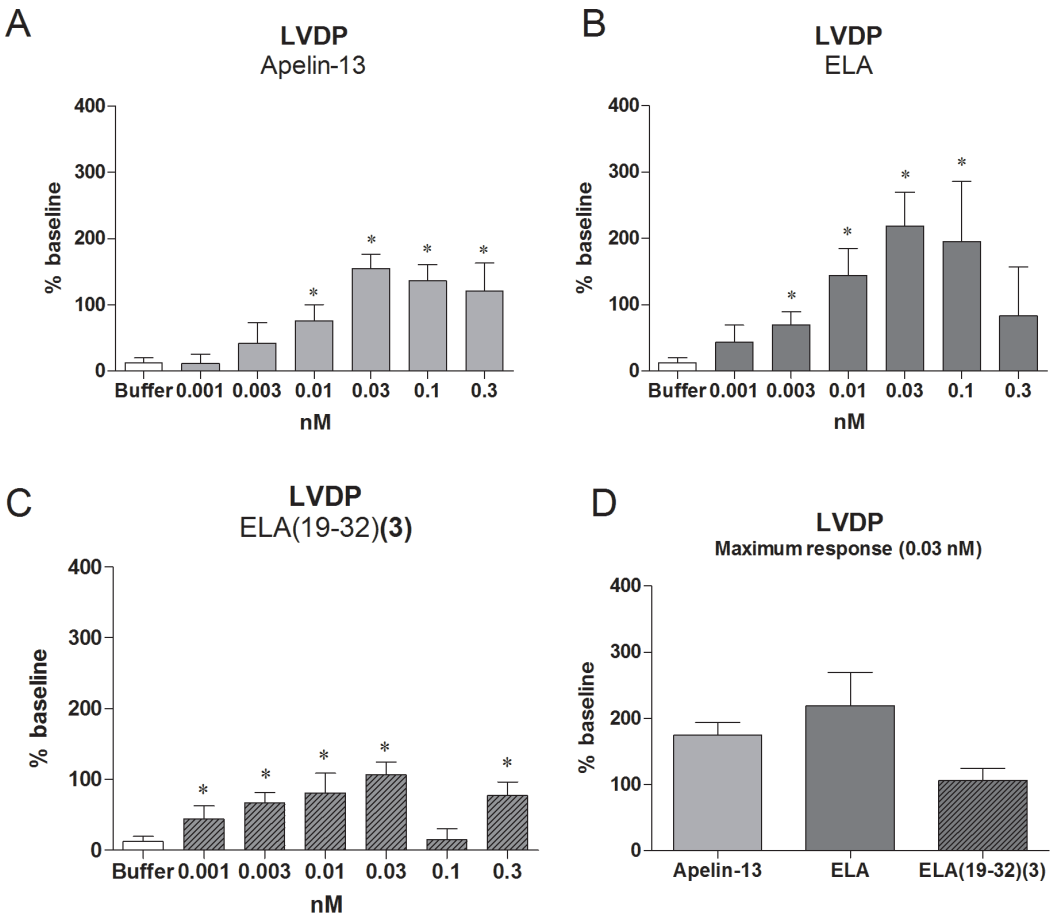

Figure 4. Left ventricular developed pressure (LVDP) of apelin-13, ELA and **3** in the Langendorff rat isolated perfused heart. Tracings depicting the LVDP induced by (**A**) apelin-13, (**B**) ELA and (**C**) **3** in rat isolated-perfused heart after administration of increasing concentrations ranging from 0.001 to 0.3 nM. (**D**) Comparison of LVDP at the maximal effective dose of 0.03 nM. Each bar represents the average value ± S.E.M from 5-6 animals. Statistical analyses were performed with a one-way ANOVA followed by Bonferroni's Multiple Comparison Test.

Figure 5

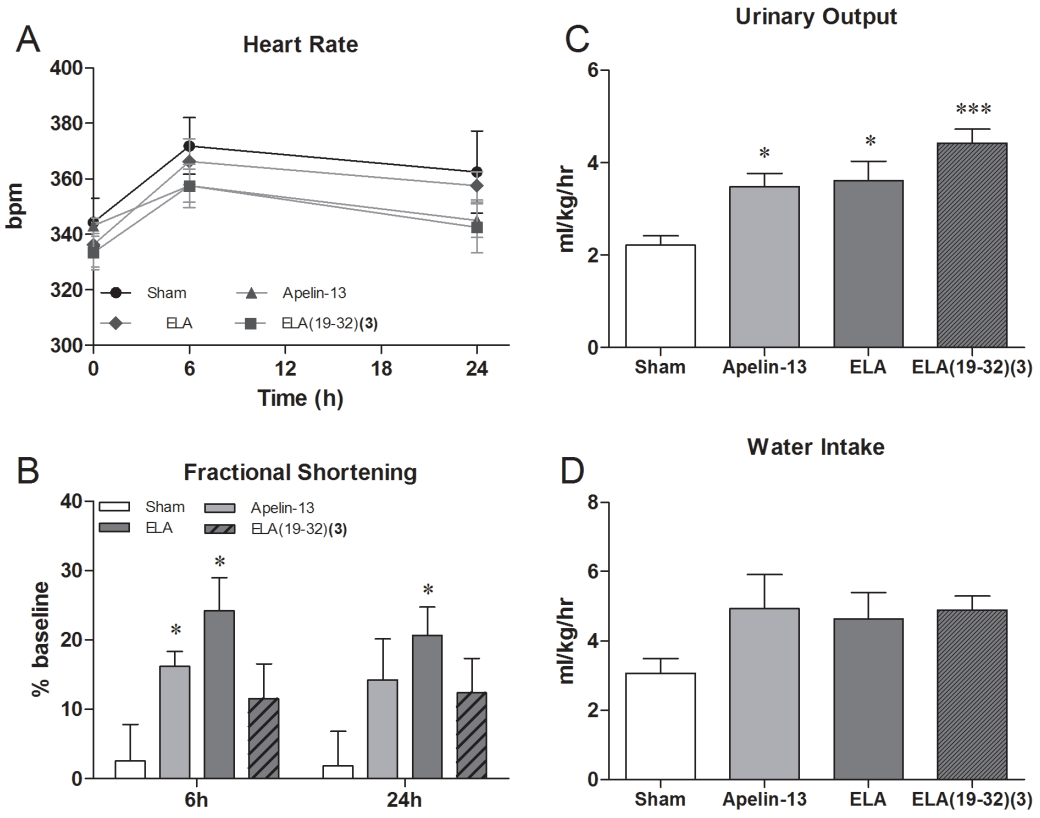

Figure 5. Impact of apelin-13, ELA and **3** on cardiac function and fluid homeostasis *in vivo* in rats. (A) Heart rate evolution assessed by echocardiography prior and 6-24 hours after peptide delivery (36 pmol/g/min) by osmotic minipump, as compared to untreated (Sham) rats. Two-way ANOVA followed by Bonferroni's Multiple Comparison Test. (B) Left ventricular fractional shortening performed by echocardiography, expressed as % of response from baseline, 6 and 24 hours after drug administration. (C) Urinary output and (D) water intake assessed by 24 hours monitoring with metabolic cage. * $p < 0.05$ vs. Sham. One way ANOVA followed by Bonferroni's Multiple Comparison Test.

Table 1. Analogue sequences, binding affinity and functional profile

N°	Sequence[a]	Binding K_i (nM)[b]	$G\alpha_{i1}$ EC_{50} (nM)[c]	β-arr2 EC_{50} (nM)[d]
Ape13	Pyr-R-P-R-L-S-H-K-G-P-M-P-F	0.37 ± 0.04	1.9 ± 0.7	68 ± 7
ELA	PyrRPVNLTMRRKLRKHNCLQRRCMPLHRSVPFP	0.19 ± 0.02	5.3 ± 2.5	45 ± 5
1	C-L-Q-R-R-C-M-P-L-H-S-R-V-P-F-P	0.23 ± 0.04	6.6 ± 2.0	151 ± 48
2	C-L-Q-R-R-C-M-P-L-H-S-R-V-P-F-P	0.34 ± 0.04	6.8 ± 2.1	106 ± 33
3	Pyr-R-R-C-M-P-L-H-S-R-V-P-F-P	0.93 ± 0.25	8.6 ± 1.2	166 ± 58
4	C-M-P-L-H-S-R-V-P-F-P	14 ± 2	15 ± 2	1064 ± 261

[a]Underlined cysteines are cyclized by a disulfide bridge. [b]Binding constants (K_i) were calculated using the Cheng-Prusoff equation and represent the concentration producing 50% competitive inhibition of binding of radioligand apelin-13[Glp^{65}, Nle^{75}, Tyr^{77}][^{125}I], values represent the mean ± SEM of three determinations. [c]Concentration that produces 50% dissociation of $G\alpha_{i1}$ subunit and, [d]50% recruitment of β-arrestin-2, as observed in BRET assay, values represent the mean ± SEM of three determinations.

Table 2. Alanine Scan and Analogues of 3, Binding Affinity and Functional Assays

N°	Sequence	Binding K_i (nM)[b]	$G\alpha_{i1}$ EC_{50} (nM)[c]	β-arr2 EC_{50} (nM)[d]
Ape13	Pyr-R-P-R-L-S-H-K-G-P-M-P-F	0.37 ± 0.04	1.9 ± 0.7	68 ± 7
ELA	PyrRPVNLTMRRKLRKHNCLQRRCMPLHRSVPFP[a]	0.19 ± 0.02	5.3 ± 2.5	45 ± 5
3	Pyr-R-R-C-M-P-L-H-S-R-V-P-F-P	0.93 ± 0.25	8.6 ± 1.2	166 ± 58
5	Pyr-R-R-C-M-P-L-H-S-R-V-P-F-**A**	11 ± 2	12 ± 2	266 ± 81
6	Pyr-R-R-C-M-P-L-H-S-R-V-P-**A**-P	49 ± 12	36 ± 10	3646 ± 1172
7	Pyr-R-R-C-M-P-L-H-S-R-V-**A**-F-P	48 ± 13	61 ± 22	5182 ± 1532
8	Pyr-R-R-C-M-P-L-H-S-R-**A**-P-F-P	20 ± 5	24 ± 6	1250 ± 336
9	Pyr-R-R-C-M-P-L-H-S-**A**-V-P-F-P	164 ± 31	147 ± 55	>10000
10	Pyr-R-R-C-M-P-L-H-**A**-R-V-P-F-P	0.14 ± 0.02	14 ± 4	82 ± 18
11	Pyr-R-R-C-M-P-L-**A**-S-R-V-P-F-P	35 ± 5	22 ± 4	1730 ± 459
12	Pyr-R-R-C-M-P-**A**-H-S-R-V-P-F-P	20 ± 3	19 ± 3	942 ± 128
13	Pyr-R-R-C-M-**A**-L-H-S-R-V-P-F-P	4.0 ± 0.9	16 ± 2	326 ± 53
14	Pyr-R-R-C-**A**-P-L-H-S-R-V-P-F-P	3.4 ± 0.6	14 ± 3	316 ± 61
15	Pyr-R-R-**A**-M-P-L-H-S-R-V-P-F-P	0.84 ± 0.12	5.7 ± 1.2	288 ± 24
16	Pyr-R-**A**-C-M-P-L-H-S-R-V-P-F-P	6.8 ± 0.6	14 ± 3	338 ± 19
17	Pyr-**A**-R-C-M-P-L-H-S-R-V-P-F-P	8.4 ± 2.2	16 ± 3	484 ± 52
18	**A**-R-R-C-M-P-L-H-S-R-V-P-F-P	0.53 ± 0.09	13 ± 3	138 ± 75
19	Pyr-R-R-C-M-P-L-H-S-R-V-P-F-P-**NH_2**	22 ± 4	20 ± 5	1423 ± 303
20	Pyr-R-R-**S**-M-P-L-H-S-R-V-P-F-P	0.37 ± 0.09	6.5 ± 2.5	229 ± 37
21	Pyr-R-R-C-**Nle**-P-L-H-S-R-V-P-F-P	0.14 ± 0.05	9.2 ± 2.7	167 ± 86

[a]Underlined cysteines are cyclized by a disulfide bridge. [b]Inhibition constants (K_i) of analogues calculated using the Cheng-Prusoff equation and representing the concentration producing 50% competitive inhibition of binding of radioligand apelin-13[Glp^{65}, Nle^{75}, Tyr^{77}][^{125}I], values represent the mean ± SEM of three determinations. [c]Concentration that produces 50% dissociation of $G\alpha_{i1}$ subunit and, [d]50% recruitment of β-arrestin-2, as observed in BRET assay, values represent the mean ± SEM of three determinations.

TABLE OF CONTENT GRAPHIC

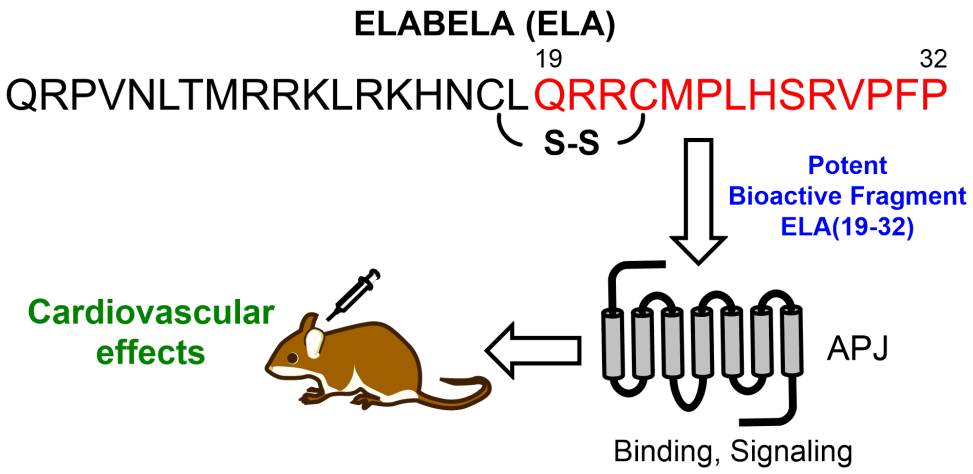

For Table of Contents only